Image Sensor-Driven Circuit Design for Measuring Optical Frequency Comb Spectrum

Yingqiu HE *
College of Science
Zhejiang University of Technology
Hangzhou, P. R. China

Kaoru MINOSHIMA
Department of Engineering Science
The University of Electro-Communications
Tokyo, Japan

Abstract

The study focuses on developing an image sensor-driven circuit for detecting light, and the circuit integrates to a spectrometer for measuring the spectral information of an optical frequency comb (OFC). The paper presents the sensor circuit design details and the spectrum measuring method. Experimental results included the analysis of the video signal for evaluating the sensor under different operating conditions and the resulting spectrum obtained from the incident OFC light. The end discusses potential points for improvement and further research.

Keywords: Image sensor, Circuit design, Optical frequency comb spectrum

1 Introduction

The optical spectrum of a light source contains information on how the optical energy or power is distributed over different wavelengths or frequencies. A pulse train generated by a mode-locked laser has a spectrum consisting of a large number of well-defined, equally spaced series of sharp lines, known as an optical frequency comb (OFC) which has been widely applied in many fields, like astronomy [1], medical diagnostics [2], precise distance measurement [3] and so on. Figure 1 shows a plot of the OFC pulses in the time domain and frequency domain, with the optical frequencies (f_{n}) are defined in $f_{\mathrm{n}} = nf_{\mathrm{rep}} + f_{\mathrm{ceo}}$, where f_{rep} is the repetition frequency producing pulses and f_{ceo} is the comb carrier-envelop offset due to the pulse-to-pulse shift. The development of OFC, like the higher of f_{rep}, opens many possibilities, including three-dimensional (3D) imaging [4]. After K. Minoshima [5] successfully demonstrated the feasibility of 3D imaging using lasers, our group [6-8] presented a novel one-shot imaging technique which utilizes an OFC-based light source to achieve high image resolution, fast processing speed, and wide dynamic range. The technique uses two image sensors to detect the spectral interference to obtain the phase difference information and then enhance the image quality. A precise optical signal detection system is therefore required.

This study aims at developing an image sensor driven circuit to detect the light and installing the circuit to a spectrometer for measuring the spectral information of OFC. The InGaAs linear image sensor [9], or line sensor, used in the study is specifically designed for near-infrared detection realizes both high-speed readout and high gain. The paper presents the sensor circuit design and the materials used in the experiments, along with an analysis of the characteristics of the video signal obtained with light from an infrared LED incident on the image sensor. This analysis also includes the impedance matching problem typically encountered in relatively high frequency circuits, as well as the performance of the video signals in relation to the integration time and conversion efficiency of the sensor. After evaluating the sensor, the paper shows the OFC spectrum obtained by installing the circuit to a spectrometer. Future work includes refining the circuit design and applying it to the 3D imaging experimental setup to im-

*The author is supported by JASSO Scholarship.

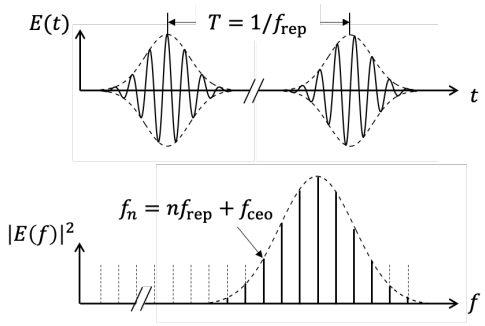

Figure 1: The diagram of the OFC presenting in the time and frequency domains.

prove performance and enable enhanced imaging capabilities within the research group.

2 Method

2.1 Designing Circuit

The InGaAs linear image sensor G11508-512SA series (hereafter referred to "sensor") used in the experiments operates by generating electric charges in its photodiodes (PDs) when light enters. These charges flow into a charge amplifier and output signals. The PD detects incident light, capturing power information for each individual pixel. The sensor consists of 2 lines, with each line containing 256 pixels. To drive the sensor, digital inputs in the form of a master clock pulse (CLK) and integration time control pulse (Reset) are required. Because two control signals must be H-COMS level inputs, one level shifter (LS) is added to change 3.3 Volts to 5.0 Volts after the function generator (FG) generating 3.3Volts. The sensor outputs an analog video signal (Video) as well as digital outputs

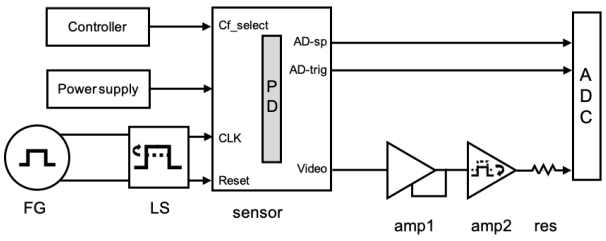

Figure 2: The diagram of the sensor-driven circuit. (amp1: buffer op-amplifier; amp2: differential op-amplifier; res: resistor)

(AD_trig, AD_sp) for sample-and-hold purposes. A buffer amplifier for enhancing sensor drive capability and a differential amplifier for compensating sensor offset voltage are needed before being fed to an oscilloscope or an analog-to-digital converter (ADC). Figure 2 displays the diagram of the circuit. Additionally, Figure 10 at the end of paper presents the schematic of the driving circuit, including the materials used.

To assess the characteristics of the sensor, the experiments follows several checking steps: (1) Output signals: The Video, AD_trig and AD_sp signals are output by employing integration then readout method. (2) Integration time: It is determined by the pulse width of the Reset signal and have an effect with Video intensity. (3) Conversion efficiency: The sensor offers two gain options: "×1" and "×10". The desired gain can be selected by controlling the Cf_select pin using external voltage. (4) Impedance Matching: The issue is a common consideration in radio frequency circuit. The output signals exhibit high impedance, necessitating the use of a buffer amplifier. Additionally, a resistor is added after the amplifiers to ensure impedance matching. These steps can help in evaluating the behavior of the sensor under different operating conditions.

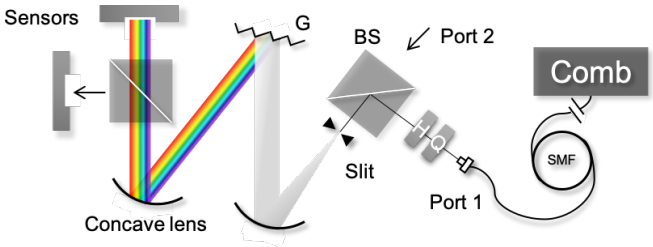

Figure 3: The diagram of the spectrometer.

2.2 Spectrometer

The Figure 3 illustrates the diagram of a spectrometer designed to measure the spectrum of an OFC. In the setup, the comb light is guided through two single mode fibers (SMFs) from two ports and detected by two sensors. The height difference between two beam light from optical table prevents their interaction. After ejecting from the fiber, a quarter-wave plate (Q) and a

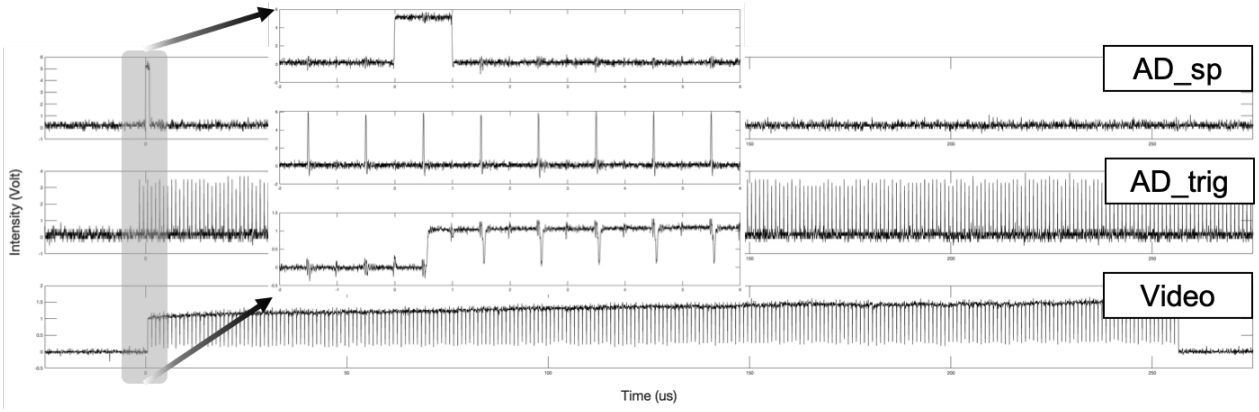

Figure 4: Overview of the output signals detected from a LED and expansion of the parts of few pixels.

half-wave plate (H) adjust the beam polarization to maximize grating efficiency. The beams then pass through a beam splitter (BS) and are shaped by a slit. Using two concave lens, each with a focal length of 100 mm, the beam is focuses before and after the diffraction grating (G) used for separating polychromatic light into the underlying constituent wavelengths. Finally, the Video outputs from the sensors is analyzed to obtain the spectrum.

To calibrate and analyze the spectrum, the setup utilizes an Optical Spectrum Analyzer (OSA). One port is connected to the OSA, while the other port remains connected to the sensor as usual. After the comb, a narrow band pass filter introduced, allowing only a single wavelength to pass through. By adjusting the pass wavelength of the filter, it becomes possible to assign each pixel of the sensor to a specific wavelength. This also allows for the determination of the resolution of the spectrum.

3 Results

3.1 Video Detected

Before installing the circuit to the spectrometer for measuring the comb spectrum, an infrared LED is used to check the circuit performance. The first step involves check the power supply line connected to the sensor. Following that, the control signal of CLK and Reset are input from the function generator to drive the sensor. Throughout the entire experiment, the frequency of CLK input to sensor is maintained at 1 MHz. As a result, the Video readout frequency is also 1 MHz, indicating that each pixel is read out in 1μs of time. After driving the sensor, Figure 4 to 7 present the results of sensor evaluations.

(1) Output signals: Figure 4 shows the output signals obtained during one complete readout period of 256 pixels. Additionally, it shows the signals form several pixels within the period, with an integration time of 0.1 ms. The maximum of intensity during test is approximately 2.8 Volts.

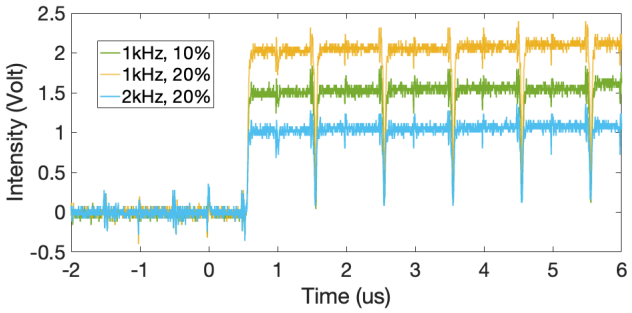

Figure 5: The Video detected with varying Reset parameters within few pixels.

(2) Integration time: By varying the frequency of Reset to 1kHz and 2kHz along with duty cycle of 10% and 20%, the integration time becomes equal to the width of Reset. The relative position of the sensor and light remains the same across the four groups. Figure 5 demonstrates that with a longer integration time, the intensity is increases, indicating that more light

can enter each pixel and the sensor's sensitivity is higher. However, this also results in a lower speed of operation.

(3) Conversion efficiency: When the Cf_select pin is connected to 5Volts or GND to, the conversion efficiency of the PD changes from "×1" to "×10". By using $\mathrm{dB} = 10\log_{10}(\times 10/\times 1)$, it is possible to calculate the gain in each pixel. Figure 6 demonstrated that the gain is 10.

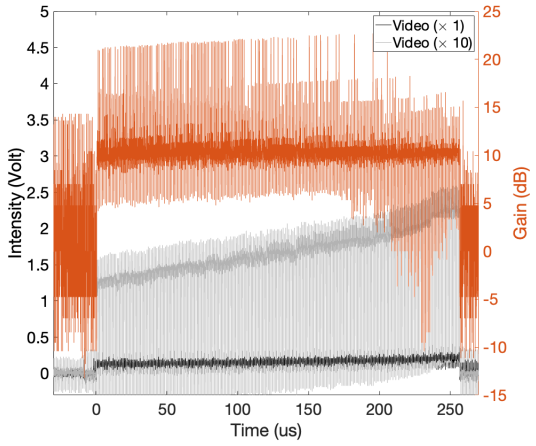

Figure 6: The Video detected with conversion efficiency of ×1 and ×10 and the calculated gain.

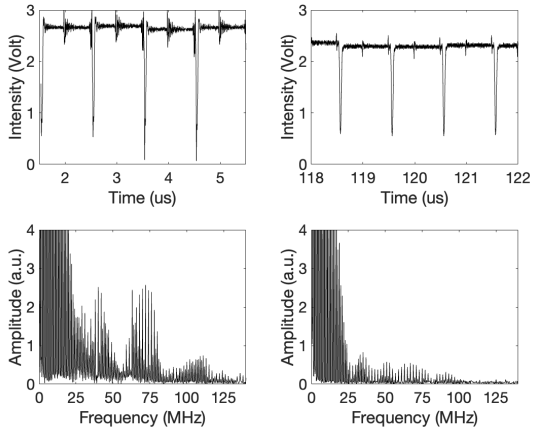

Figure 7: The Video detected without (left) and with (right) the resistor within few pixels and its spectrum.

(4) Impedance matching: The issue is a common consideration in radio frequency circuit. A resistor used here to match the impedance after the amplifiers. The Video is then measured both without and with the resistor, and their frequency spectra are compared using FFT in MATLAB. In Figure 7, the left side shows strong harmonic frequencies around 40MHz, 70MHz and 110MHz, but after adding a resistor, the right side of the figure demonstrates that only a small intensity of high frequency signals remains. This indicates that the resistor helps mitigate the presence of unwanted harmonics.

3.2 Spectrum Measured

4 Discussion

The results reveal that the presence of residual unwanted signals in the Video output. To address this issue, several improvements are proposed, including using a power supply line with higher sufficiency ability to draw current and inserting an RC filter after the amplifier output to reduce noise. Future work for the circuit includes using an FPGA (Field-Programmable Gate Array) for pulse generation instead of a function generator and to analyze the Video output instead of relying on an oscilloscope.

The goal of this study is to measure the spectrum of the OFC in a spectrometer setup rather than using OSA. This choice was motivated by the final goal of the setup, which is to use it for measuring the spectral interference pattern of two beams and analyze the phase difference between them. The phase difference information is then used to give feedback to the OFC. Besides, the ultimate objective of the research group is to achieve a higher quality of 3D imaging, and all the mentioned improvements and approaches were aimed at this goal. For more detailed information on the techniques and methods employed, please refer to reference [8].

5 Conclusions

In conclusion, this study effectively developed an image sensor driven circuit for detecting incident light and applied it into a spectrometer for measuring the OFC spectrum. The obtained spectrum results exhibited good performance, achieving a resolution of 1 nm per pixel. The testing circuit results provided insights into driving the sensor under various conditions, like

integration time and conversion efficiency. The study also addressed the important aspect of impedance matching in the circuit design. Overall, it is hoped that this study can contribute positively to the research group's goals and objectives.

6 Acknowledgments

The author expresses gratitude to JASSO scholarship, Prof. Kaoru Minishima for lab research opportunity, and Takashi Kato-sensei, Yasushi Nekoshima, Keito Hino, Haochen Tian for experimental assistance. Special thanks to the lab, the JUSST program, and the Aikido club members.

References

[1] M. Andrew, A. Tyler et al, "Stellar spectroscopy in the near-infrared with a laser frequency comb", *Optica* 6, 233-239, 2019.

[2] J.T. Michael et al, "Cavity-enhanced optical frequency comb spectroscopy: application to human breath analysis", *Optics Express* 16, 2387-2397, 2008.

[3] E.D. Caldwell, L.C. Sinclair, N.R. Newbury et al, "The time-programmable frequency comb and its use in quantum-limited ranging", *Nature* 610, 667-673, 2022.

[4] E. Vicentini, Z. Wang, K. Van Gasse et al, "Dual-comb hyperspectral digital holography", *Nat. Photon.* 15, 890-894, Nov. 2021.

[5] K. Minoshima et al, "Simultaneous 3-D Imaging Using Chirped Ultrashort Optical Pulses", *Jpn. J. Appl. Phys.* 33 L1348, 1994.

[6] T. Kato, M. Uchida, Y. Tanaka, K. Minoshima, "Non-scanning three-dimensional imaging using two-dimensional spectroscopy and spectral interferometry with a chirped frequency comb", CLEO-PR, Singapore, 2017, pp. 1-2.

[7] T. Kato, M. Uchida, Y. Tanaka, K. Minishoma, "High-resolution 3D imaging method using chirped optical frequency combs based on convolution analysis of the spectral interference fringe", *OSA Continuum* Vol. 3, No. 1, 15 Jan. 2020.

[8] T. Kato, H. Ishii, K. Terada, T. Morito, K. Minoshima, "Fully non-scanning three-dimensional imaging using an all-optical Hilbert transform enabled by an optical frequency comb", arXiv: 2006.07801 [physics.optics], Jun. 2020.

[9] `https://www.hamamatsu.com/us/en/product/optical-sensors/image-sensor/ingaas-image-sensor/ingaas-linear-image-sensor/G11508-512SA.html`

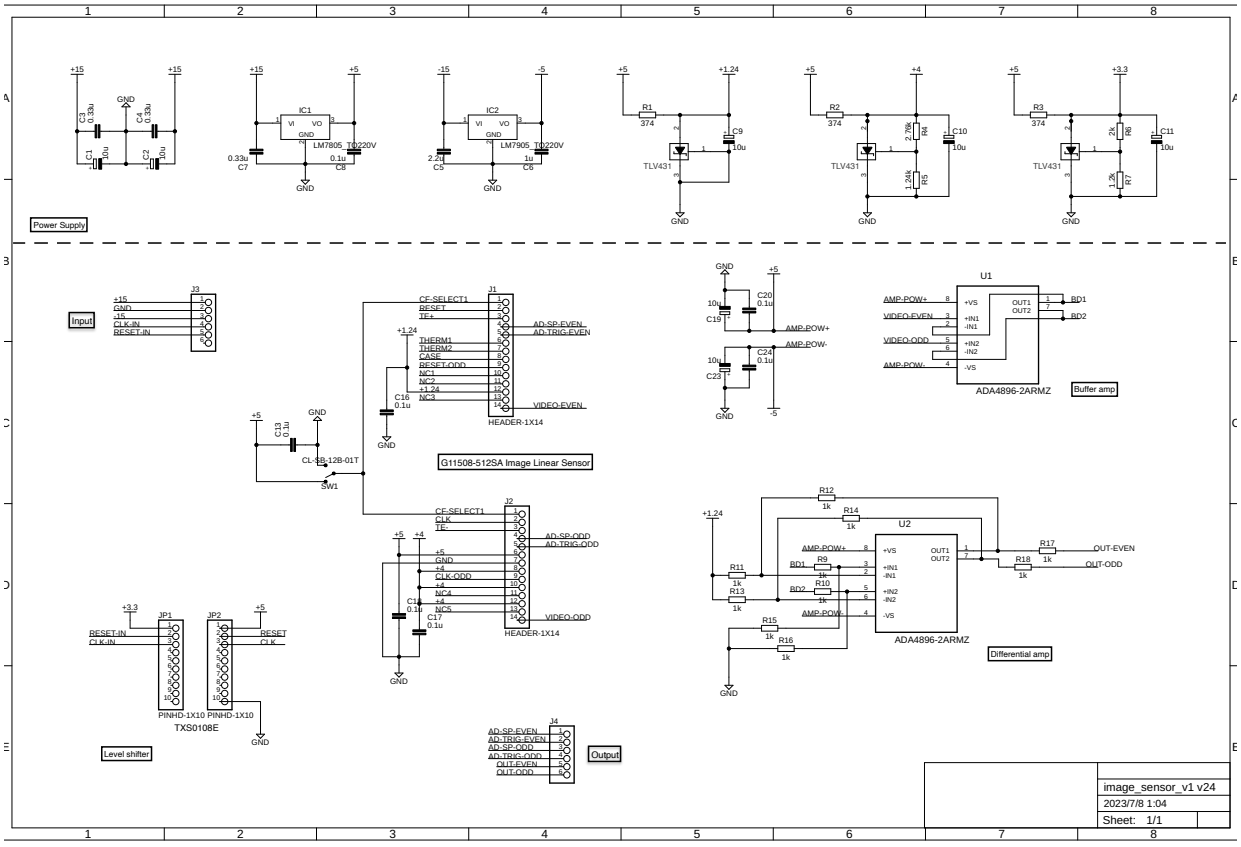

Figure 8: Schematic of the circuit.